SPE 154448

Transient Gas Flow in Unconventional Gas Reservoirs

Yu-Shu Wu, SPE, Colorado School of Mines, Cong Wang, SPE, Colorado School of Mines,Jianfang Li, SPE, RIPED of PetroChina, and Perapon Fakcharoenphol, SPE, Colorado School of Mines

This paper was prepared for presentation at the EAGE Annual Conference & Exhibition incorporating SPE Europec held in Copenhagen, Denmark, 4–7 June 2012.

Abstract

Unconventional gas resources from low-permeability formation, i.e., tight and shale gas, are currently received great attention because of their potential to supply the world with sufficient energy for decades to come. In the past few years, as a result of industry-wide R&D effort, progresses are being made towards commercial development of gas and oil from such unconventional resources. However, studies, understandings, and effective technologies needed for development of unconventional reservoirs are far behind the industry needs, and gas recovery from those unconventional resources remains low (estimated at 10-30% of GIP).

Gas flow in low-permeability unconventional reservoirs is highly nonlinear, coupled by many co-existing processes, e.g., non-Darcy flow and rock-fluid interaction within tiny pores or micro-fractures. Quantitative characterization of unconventional reservoirs has been a significant scientific challenge currently. Because of complicated flow behavior, strong interaction between fluid and rock, the traditional Darcy law may not be applicable for describing flow phenomena in general. In this paper, we will discuss a general mathematical model of gas flow through unconventional porous media and use both numerical and analytical approaches to analyze gas flow in unconventional reservoirs. In particular, we will present analytical and numerical solutions of incorporating Klinkenberg effect, non-Darcy flow with threshold pressure gradient, and flow behavior in pressure sensitive media. We will discuss the numerical implementation of the mathematical model and show applications of the mathematical model and solutions in analyzing transient gas flow in conventional reservoirs.

Introduction

This paper presents our continual effort in developing simulation models and tools for unconventional gas reservoirs (Wu and Fackahroenphol, 2011). As unconventional gas resources from low-permeability reservoirs are receiving great attention in the world, many studies and progresses are being made towards commercial development of gas and oil from these unconventional resources (Denny, 2008; Bybee, 2008; King, 2010). However, our understandings of gas flow and effective tools for effective development of unconventional reservoirs are far behind the industry needs (Wu et al. 2009). Unlike flow in traditional reservoir s, nanoscale observations and field data analysis tell us that gas flow in such extremely low-permeability formations is complicated by flow condition and many co-existing processes, such as severe heterogeneity on any scales, Klinkenberg effect or known as Knudsen diffusion (Klinkenberg, 1941), non-Darcy flow behavior (Wu, 2002), adsorption/desorption (Silin and Kneafsey, 2011), strong interactions between fluid (gas and water) molecules and solid materials within tiny pores (Severino et al. 2010) as well as micro- and macro- fractures of shale and tight formations (Shabro et. al. 2011). As a result, there is a general lack in technologies or approaches available for effective gas production from unconventional reservoirs (MIT, 2010) or effective and applicable reservoir simulation technologies currently available and few modeling efforts (Kelkar and Atiq, 2010).

Currently, there is little analysis of what the effect of Klinkenberg effect, non-Darcy flow behavior and adsorption/desorption terms is in flow and well tests in unconventional gas reservoirs. In order to study transient gas flow and provide type curves for well testing analysis, an accurate unconventional reservoir simulator should be built considering both the nonlinear flow and natural/hydraulic fractures (Wu and Fackahroenphol, 2011). Some related studies using double-porosity or discrete fractures model (DFM) are carried out for fracture modeling (Mirzaei and Cipolla, 2011; Gong et al. 2011; Wu et al. 2009).

This paper presents a two-phase flow model for simulating both gas and water flow in shale oil/gas and tight gas reservoirs. Single-phase gas flow is handled as a special case of the proposed model and used for transient flow and well testing analysis. The two-phase flow model incorporates many of the key nonlinear gas physical processes in unconventional reservoirs, such as non-Darcy flow, Klinkenberg effect, and sorption. In addition, we have derived several analytical solutions for gas flow through unconventional porous medi, which are used for verifying the numerical model formulation and results. The mathematical model has been implemented into a multiphase, multidimensional reservoir simulator (Wu, 2000). The proposed numerical modeling approach is suitable for modeling various types of shale and gas reservoirs, including discrete-hybrid- double-, and other multiple-continuum conceptual models for multi-scaled fractures and matrix systems and various flow domains. The simulator can be used for quantitative studies of transient gas flow behavior as well as well testing analysis. As an application example, the model is used to generate several transient flow curves in terms of the pseudo gas pressure and dimensionless time.

Flow Model

A multiphase system of gas and water in a porous or fractured unconventional reservoir is assumed to be similar to the black oil model, composed of two phases: gaseous and aqueous phases. For simplicity, the gas and water components are assumed to be present only in their associated phases, and adsorbed gas is within the solid phase of rock. Each fluid phase flows in response to pressure, gravitational, and capillary forces according to the multiphase extension of Darcy law or several non-Darcy laws, discussed below. In an isothermal system containing two mass components, subject to flow and sorption, two mass-balance equations are needed to fully describe the system, as described in an arbitrary flow region of a porous or fractured domain for flow of phase β (β = g for gas and β = w for water),

$$\frac{\partial}{\partial t}(\phi S_\beta \rho_\beta + m_k) = -\nabla \bullet (\rho_\beta \mathbf{v}_\beta) + q_\beta \tag{1}$$

where ρ_β is the density of fluid β; $\mathbf{v}_\beta$ is the volumetric velocity vector of fluid β; S_β is the saturation of fluid β; ϕ is the effective porosity of formation; t is time; m_k is the adsorption or desorption term for gas component (k=g only) per unit volume of formation; and q_β is the sink/source term of phase (component) β per unit volume of formation,

The flow velocity in Eq. (1) will be evaluated (1) using the Darcy's law with Klinkenberg effects (for gas flow); (2) using the nonlinear flow models to describe non-Darcy flow behavior (e.g., Wu, 2002); and (3) flow condition where flow may not occur until the pressure or potential gradient reaches a certain threshold value (Wu and Pruess, 1998). Specifically, $\mathbf{v}_\beta$ is the flow velocity (or volumetric flow rate) in Eq. (1), defined differently under different flow regimes or situations, as discussed in the following.

Darcy's Flow: When the Darcy's law is applicable, the velocity, $\mathbf{v}_\beta$, is defined as,

$$\mathbf{v}_\beta = -\frac{k k_{r\beta}}{\mu_\beta}\left(\nabla \Phi_\beta\right) \tag{2}$$

where k is the absolute permeability of the porous media, treated as a function of gas pressure with Klinkenberg effect accounted for; $k_{r\beta}$ is relative permeability to phase β, treated as a function of fluid saturation; μ_β is the viscosity of phase β as a function of pressure; and $\nabla \Phi_\beta$ is flow potential gradient, defined as,

$$\nabla \Phi_\beta = \left(\nabla P_\beta - \rho_\beta g \nabla D\right) \tag{3}$$

where P_β is the pressure of phase β; g is gravitational acceleration constant; and D is the depth from a datum.

Non-Darcy's Flow: In addition to multiphase Darcy flow, non-Darcy flow may also occur between and among the continua in tight or shale gas reservoirs. The flow velocity, $\mathbf{v}_\beta$, for non-Darcy flow of each fluid may be described using the multiphase extension of the *Forchheimer* equation (e.g., Wu, 2002),

$$-\left(\nabla\Phi_\beta\right)=\frac{\mu_\beta}{k_{r\beta}}k\,\mathbf{v}_\beta+\beta_\beta\rho_\beta\mathbf{v}_\beta\left|\mathbf{v}_\beta\right| \tag{4}$$

where β_β is the effective non-Darcy flow coefficient with a unit m^{-1} for fluid β under multiphase flow conditions.

Flow with Threshold Pressure Gradient: The phenomenon of flow with threshold-pressure-gradient concept has been observed in laboratory and is commonly used to describe nonlinear flow behavior in low permeability reservoirs (Xiong et al. 2008; Lei et al. 2007). This flow condition is similar to Bingham non-Newtonian flow through porous media (Wu and Pruess, 1998), which is used in this work to describe conditions where flow may not occur until the pressure or potential gradient reaches a certain threshold value. Instead of introducing an apparent viscosity for Bingham fluid, an effective potential gradient approach, as follows, has been proven to be more efficient numerically (Wu et al., 1992). Using the effective potential gradient, the flow of gas or liquid in a low-permeability reservoir is described by,

$$\mathbf{v}_\beta=-\frac{kk_{r\beta}}{\mu_\beta}\left(\nabla\Phi_e^\beta\right) \tag{5}$$

where $\mu_{b,\beta}$ is the Bingham plastic viscosity coefficient for phase β; and $\nabla\Phi_e^\beta$ is the effective potential gradient whose scalar component in the x direction (the flow direction) is defined as,

$$\left(\nabla\Phi_e\right)_x=\left(\nabla\Phi\right)_x-G \quad \text{for} \quad \left(\nabla\Phi\right)_x>G \tag{6a}$$

$$\left(\nabla\Phi_e\right)_x=\left(\nabla\Phi\right)_x+G \quad \text{for} \quad \left(\nabla\Phi\right)_x<-G \tag{6b}$$

$$\left(\nabla\Phi_e\right)_x=0 \quad \text{for} -G<\left(\nabla\Phi\right)_x<G \tag{6c}$$

where G is the threshold (or minimum) potential gradient for the fluid to become mobile.

Adsorption: Natural gas can be present as a free gas phase or as adsorbed gas on solids in pores. In shales, methane molecules are adsorbed mainly to the carbon-rich components, i.e. kerogen (Silin and Kneafsey, 2011). As observed, adsorbed mass of gas can provide significant fraction of gas reserves and recovery. As the pressure decreases with gas production from reservoirs, more adsorbed gas is released from solid to free gas phase, contributing to the total production. In our model, the mass of adsorbed gas in formation volume V is described (Alana, 2011):

$$m_g(V)=\rho_K\rho_g f(p)\overline{S_k}V \tag{7}$$

where ρ_K is kerogen density, ρ_g is gas density at standard condition, $\overline{S_k}$ is the average volume relative of kerogen in bulk volume, $m_g(V)$ is the adsorbed gas mass in bulk formation volume V. In Eq. (7), f(P) is the adsorption isotherm function. If the adsorbed gas molecules form a thin layer on the solid surface, adsorption terms can be well represented by the Langmuir isotherm (Langmuir, 1916), as shown in **Fig. 1**, which describes the dependency of adsorbed gas volume on pressure at constant temperature.

$$f(P)=\frac{V_L P_g}{P_g+P_L} \tag{8}$$

where, V_L is the Langmuir volume (the maximum adsorption capacity at a given temperature), and P_L is the Langmuir pressure (the pressure at which the adsorbed gas content is equal to $\frac{V_L}{2}$).

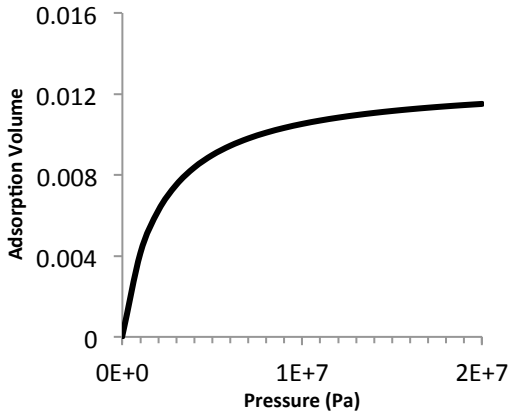

Fig. 1 Gas adsorption volume per mass of rock at standard condition with pressure

Klinkenberg Effect: In low-permeability formation or under low pressure condition, the Klinkenberg effect (Klinkenberg, 1941) may be too significant to be ignored when modeling gas flow in reservoirs (Wu et al. 1998). Klinkenberg effect is expected to be larger in unconventional reservoirs, because of small size pores and low permeability associated. Under such flow conditions, absolute permeability for the gas phase is written as a function of gas pressure as,

$$k_g = k_\infty \left(1 + \frac{b}{P_g}\right) \tag{9}$$

where k_∞ is constant, absolute gas-phase permeability under very large gas-phase pressure (where the Klinkenberg effect is minimized); and b is the Klinkenberg factor, depending on the pore structure of the medium and formation temperature.

Numerical Model

As discussed above, the PDE that governs gas flow in gas reservoirs is nonlinear. In addition, gas flow in unconventional reservoirs is subject to many other nonlinear flow processes. In general, the flow model is solved using a numerical approach. This work follows the methodology for reservoir simulation, i.e., using numerical approaches to simulate gas and water flow, following three steps: (1) spatial discretization of mass conservation equations; (2) time discretization; and (3) iterative approaches to solve the resulting nonlinear, discrete algebraic equations.

Discrete Equations: The component mass-balance Equations (Eq.1) are discretized in space using a control-volume or integrated finite difference concept (Pruess et at. 1999), as shown in **Fig. 2**. The control-volume approach provides a general spatial discretization scheme that can represent a one-, two- or three-dimensional domain using a set of discrete meshes. Each mesh has a certain control volume for a proper averaging or interpolation of flow and transport properties or thermodynamic variables. Time discretization is carried out using a backward, first-order, fully implicit finite-difference scheme. The discrete nonlinear equations for components of gas and water at gridblock or node i can be written in a general form:

$$\left\{M_i^{k,n+1} - m_i^{k,n+1}\Delta t - M_i^{k,n}\right\}\frac{V_i}{\Delta t} = \sum_{j\in\eta_i} flow_{ij}^{k,n+1} + Q_i^{k,n+1} \tag{10}$$

(k = 1, 2) and (i=1, 2, 3, …, N)

where superscript k serves also as an equation index for gas and water components with k = 1 (gas) and 2 (water); superscript n denotes the previous time level, with n+1 the current time level to be solved; subscript i refers to the index of gridblock or node i, with N being the total number of nodes in the grid; Δt is time step size; V_i is the volume of node i; η_i contains the set of direct neighboring nodes (j) of node i; M_i^k, m_i^k, $flow_{ij}^k$, and Q_i^k are the accumulation and reaction (absorption or desorption) terms, respectively, at node i; the component mass "flow" term between nodes i and j, and sink/source term at node i for component k, respectively, defined below.

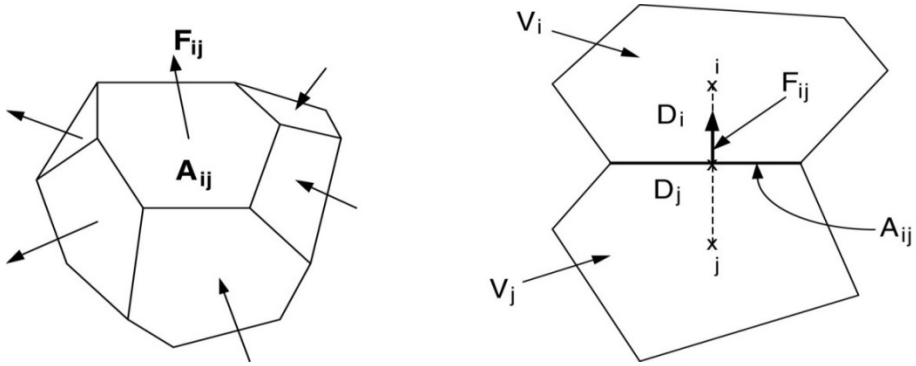

Fig. 2 Space discretization and flow-term evaluation in the integral finite difference method (Pruess et al. 1999)

The "flow" terms in Eq. (10) are mass fluxes by advective processes and are described by a discrete version of Darcy's law, i.e., the mass flux of fluid phase β along the connection is given by

$$\text{flow}_{\beta,ij} = \lambda_{\beta,ij+1/2}\gamma_{ij}\left(\Phi_{\beta j} - \Phi_{\beta i}\right) \tag{11}$$

where $\lambda_{\beta,i\,j+1/2}$ is the mobility term to phase β, defined as

$$\lambda_{\beta,i\,j+1/2} = \left(\frac{\rho_\beta k_{r\beta}}{\mu_\beta}\right)_{ij+1/2} \tag{12}$$

In Eq. (12), γ_{ij} is transmissivity and is defined as (Pruess et al. 1999),

$$\gamma_{ij} = \frac{A_{ij}k_{ij+1/2}}{D_i + D_j} \tag{13}$$

where A_{ij} is the common interface area between the connected blocks or nodes i and j (**Fig. 2**); D_i is the distance from the center of block i to the common interface of blocks i and j; and $k_{ij+1/2}$ is an averaged (such as harmonic-weighted) absolute permeability along the connection between elements i and j. The flow potential term in Eq. (11) is defined as,

$$\Phi_{\beta i} = P_{\beta i} - \rho_{\beta,ij+1/2}\, g\, Z_i \tag{14}$$

where Z_i is the depth to the center of block i from a reference datum.

Handling fractured media: to implement fractured modeling approaches, special attention is needed to calculate fracture-matrix mass transfer. Commonly used double-porosity and dual-permeability models use a quasi-steady state assumption for handling fracture-matrix interaction. In this work, the flow between fractures and matrix is still evaluated using Eq. (11); however, the transmissibility for the fracture-matrix flow is given by,

$$\gamma_{ij} = \frac{A_{FM}k_M}{l_{FM}} \tag{15}$$

where A_{FM} is the total interface area between fractures and matrix of element i and j (one of them is a fracture and the other is a matrix blocks); k_M is matrix absolute permeability; and l_{FM} is a characteristic distance or equivalent length for flow between fracture and matrix blocks. It can be calculated from ideal one-, two, and three-dimensional rectangular matrix block under quasi-steady state flow.

Handling Klinkenberg effect: To include the Klinkenberg effect on gas flow, the absolute permeability to gas phase in (13) should be evaluated using Eq. (9) as a function of gas phase pressure.

Handling "non-Newtonian" flow: In the case that gas or water flow is subject to a threshold potential gradient, the discrete potential gradient in (11) should be replaced by the effective potential gradient, Eq. (6) for phase flow term evaluation.

Handling non-Darcy flow: Under the non-Darcy flow condition of Eq. (4), the flow term ($\mathrm{flow}_{\beta,ij}$) in Eq. (11) along the connection (i, j), between elements i and j, is numerically defined as (Wu, 2002),

$$\mathrm{flow}_{\beta,ij} = \frac{A_{ij}}{2\left(k\beta_\beta\right)_{ij+1/2}}\left\{-\frac{1}{\lambda_\beta}+\left[\left(\frac{1}{\lambda_\beta}\right)^2-\bar{\gamma}_{ij}\left(\Phi_{\beta j}-\Phi_{\beta i}\right)\right]^{1/2}\right\} \tag{16}$$

in which the non-Darcy flow transmissivity is defined as,

$$\bar{\gamma}_{ij} = \frac{4\left(k^2\rho_\beta\beta_\beta\right)_{ij+1/2}}{D_i + D_j} \tag{17}$$

In evaluating the "flow" terms in the above Eqs. (11)-(17), subscript ij+1/2 is used to denote a proper averaging or weighting of fluid flow properties at the interface or along the connection between two blocks or nodes i and j. The convention for the signs of flow terms is that flow from node j into node i is defined as "+" (positive) in calculating the flow terms.

Eq. (10) presents a precise form of the balance equation for each mass component of gas and water in a discrete form. It states that the rate of change in mass accumulation (plus adsorption or desorption, if existing) at a node over a time step is exactly balanced by inflow/outflow of mass and also by sink/source terms, when existing for the node. As long as all flow terms have the flow from node i to node j equal to and opposite to that of node j to node i for fluids, no mass will be lost or created in the formulation during the solution. Therefore, the discretization in Eq. (10) is conservative.

Numerical Solution

In this work, we use the fully implicit scheme to solve the discrete nonlinear Eq. (10) with a Newton iteration method. Let us write the discrete nonlinear equation, Eq. (10), in a residual form as,

$$R_i^{k,n+1} = \left\{M_i^{k,n+1} + \Delta t\, m_i^{k,n+1} - M_i^{k,n}\right\}\frac{V_i}{\Delta t} - \sum_{j\in\eta_i}\mathrm{flow}_{ij}^{k,n+1} - Q_i^{k,n+1} = 0 \tag{18}$$

$(k = 1, 2;\ i = 1, 2, 3, \ldots, N)$.

Eq. (18) defines a set of 2×N coupled nonlinear equations that need to be solved for every balance equation of mass components, respectively. In general, two primary variables per node are needed to use the Newton iteration for the associated two equations per node. The primary variables selected are gas pressure and gas saturation. The rest of the dependent variables, such as relative permeability, capillary pressures, viscosity and densities, adsorption term, as well as nonselected pressures, and saturation,—are treated as secondary variables, which are calculated from selected primary variables.

In terms of the primary variables, the residual equation, Eq. (18), at a node i is regarded as a function of the primary variables at not only node i, but also at all its direct neighboring nodes j. The Newton iteration scheme gives rise to

$$\sum_m \frac{\partial R_i^{k,n+1}\left(x_{m,p}\right)}{\partial x_m}\left(\delta x_{m,p+1}\right) = -R_i^{k,n+1}\left(x_{m,p}\right) \tag{19}$$

where x_m is the primary variable m with m = 1 and 2, respectively, at node i and all its direct neighbors; p is the iteration level; and i =1, 2, 3, …, N. The primary variables in Eq. (19) need to be updated after each iteration,

$$x_{m,p+1} = x_{m,p} + \delta x_{m,p+1} \tag{20}$$

The Newton iteration process continues until the residuals $R_i^{k,n+1}$ or changes in the primary variables $\delta x_{m,p+1}$ over iteration are reduced below preset convergence tolerances.

Numerical methods are generally used to construct the Jacobian matrix for Eq. (19), as outlined in Forsyth et al. (1995). At each Newton iteration, Eq. (19) represents a system of (2×N) linearized algebraic equations with sparse matrices, which are solved by a linear equation solver.

Analytical Solution

In this section, we present several analytical solutions for steady-state gas flow in unconventional reservoirs with considering the Klinkenberg effect and non-Darcy flow. We also use analytical solutions for transient flow with Klinkenberg effect. In general, the gas flow governing equation with Klinkenberg effect and non-darcy flow needs to be solved by a numerical method. However, under 1-D flow, it is possible to obtain certain analytical solutions of steady-state or transient state, as proven in the following flow conditions. Detailed derivation processes for the steady-state solutions are provided in the Appendix A.

Klinkenberg Effect Steady-State Flow: Under horizontal and steady-state flow conditions, Equations for flow with Klinkenberg effect can be simplified as:

Klinkenberg effects: $$k = k_\infty\left(1+\frac{b}{P}\right) \quad (21.a)$$

Mass conservation equation: $$\rho v A = Q_m \quad (21.b)$$

Darcy's Law: $$v = -\frac{k}{\mu}\nabla P \quad (21.c)$$

Ideal gas equation: $$\rho = \alpha P \quad (21.d)$$

Detailed description of the model and derivation process can be seen in the Appendix A.

Solution for 1-D linear flow is: $$P(x) = -b + \sqrt{b^2 + P_L^2 + 2bP_L + \frac{2Q_m\mu(L-x)}{k_\infty A\alpha}} \quad (22)$$

Solution for 1-D radial flow is: $$P(r) = -b + \sqrt{b^2 + P_e^2 + 2bP_e + \frac{2Q_m\mu}{2\pi h\alpha k_\infty}\ln\left(\frac{r_e}{r}\right)} \quad (23)$$

Klinkenberg Effect in Transient Flow Under horizontal radial flow towards a well, approximated as a line source/sink, in an infinite, uniform, and horizontal formation, the gas flow equation and solution could be expressed in terms of P_b^2 (Wu et al. 1998),

$$\frac{1}{r}\frac{\partial}{\partial r}\left(r\frac{\partial P_b^2}{\partial r}\right) = \frac{1}{\omega}\frac{\partial P_b^2}{\partial t}, \quad (24)$$

$$P_b^2(r,t) = P_{bi}^2 - \frac{\mu Q_m}{2\pi kh\alpha}\mathrm{Ei}\left(-\frac{r^2}{4\omega t}\right) \quad (25)$$

where: $$P_b = P + b \quad (26)$$

$$\omega = \frac{kP_b}{\Phi\mu} \quad (27)$$

Non-Darcy Flow Steady-State Flow: Under horizontal and steady-state flow condition, Equations for non-darcy flow with can be simplified as:

Mass conservation equation: $$\rho v A = Q_m \quad (28.a)$$

Forchheimer flow: $$-\nabla P = \frac{\mu}{k}v + \beta\rho v|v| \quad (28.b)$$

Ideal gas equation: $$\rho = \alpha P \quad (28.c)$$

Solution for linear flow is: $$P_x = \sqrt{\frac{c_1^2+2c_1\frac{\mu}{k}}{2\alpha\beta}(L-x)+P_L^2} \quad (29)$$

Solution for radial flow is: $$P_r = \sqrt{P_L^2 - \frac{c_2^2}{2\alpha\beta}\left(\frac{1}{r}-\frac{1}{r_e}\right)+\frac{c_2\mu}{k\alpha\beta}\ln\left(\frac{r_e}{r}\right)} \quad (30)$$

Model Verification

This session is to examine the accuracy of our simulator formulation in simulating porous medium gas flow with the Klinkenberg effect and non-Darcy flow. The problem concerns steady-state and transient gas flow across a 1-D reservoir. The system contains steady/transient-state gas flow at an isothermal condition and a constant gas mass injection/production rate is imposed at one side of the rock or well. The other boundary of the rock/reservoir is kept at constant pressure. Eventually, the system will reach steady state, if the production is maintains for a long period of time. A comparison of the pressure profiles along the rock block from the simulation and the exact, analytical solution is shown in **Figs. 3-8,** indicating that our simulated pressure distribution is in excellent agreement with the analytical solutions for all the problems of 1-D linear or 1-D radial flow with Klenkenberg effect or non-Darcy flow. The input parameters used in the calculations are provided in **Table 1**.

Table. 1 Parameters for Gas Flow Verification

Parameter	Value	Unit
Porosity	$\varphi = 0.3$	
Permeability	$k_\infty = 5\times10^{-19}$	m^2
klinkenberg coefficient	$b = 7.6\times10^5$	Pa
	$b = 7.6\times10^4$	
	$b = 7.6\times10^6$	
compressibility factor	$\alpha = 1.18\times10^{-5}$	kg/Pa m^3
gas viscosity	$\mu = 1.84\times10^{-5}$	Pa s
formation temperature	$T = 25$	℃
gas mass injection rate	$Q_m = 1\times10^{-6}$	kg/s
outlet boundary pressure	$P_L = 1\times10^5$	Pa
cross-area	A=1	m^2
model height	H=1	M
outlet radius	$r_e = 10$	M
well radius	$r_w = 0.1$	M
non-Darcy flow constant	$c_\beta = 6.2\times10^{-3}$	$m^{1.5}$
	$c_\beta = 6.2\times10^{-4}$	
	$c_\beta = 6.2\times10^{-5}$	
	$\beta = c_\beta/(k^{1.25}\Phi^{0.75})$	
transient flow time	1	days
	10	
	100	

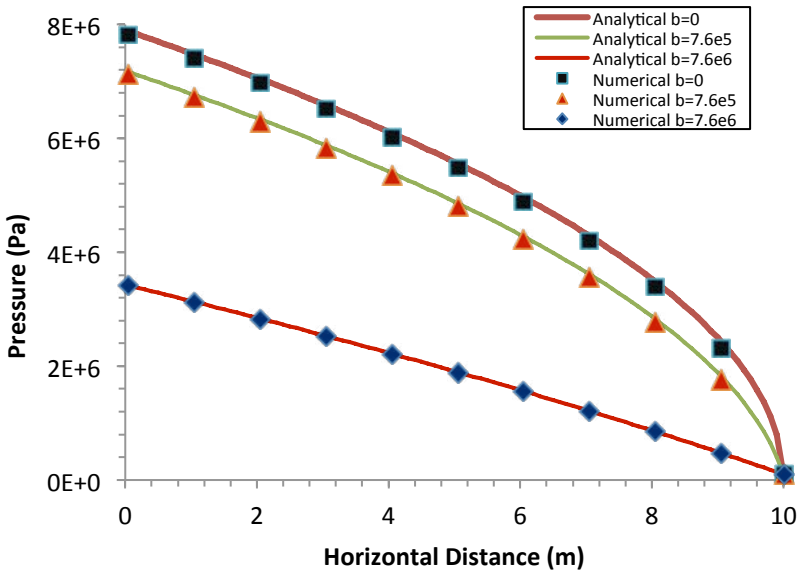

Fig. 3 Steady-State Analytical and Numerical Results for Linear Gas Flow with Klinkenberg Effect

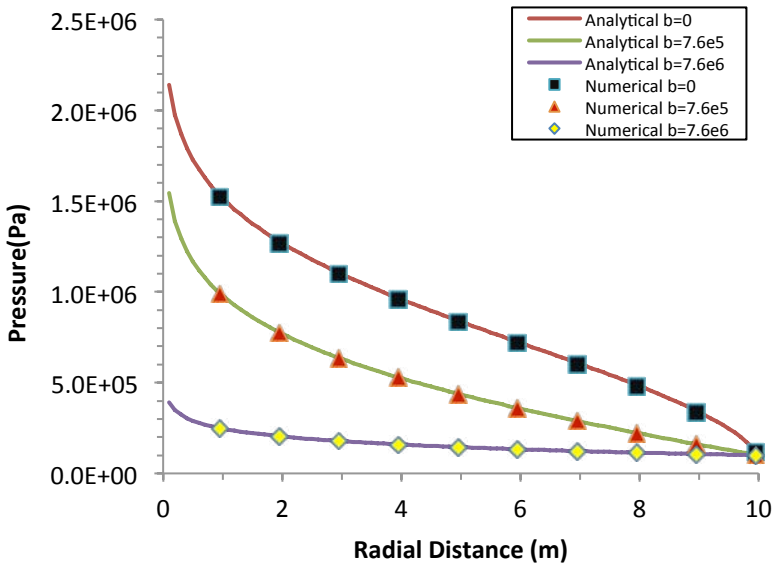

Fig. 4 Steady-State Analytical and Numerical Results for Radial Gas Flow with Klinkenberg Effect

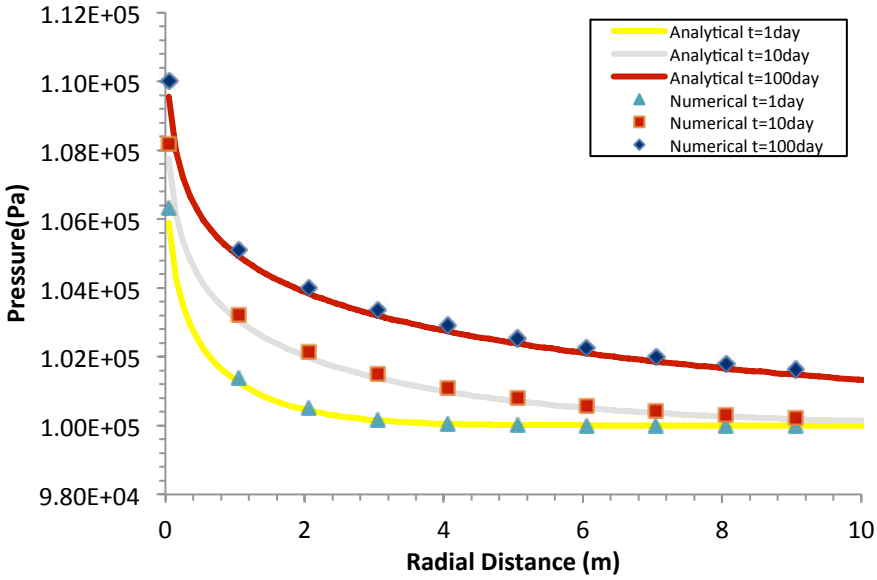

Fig. 5 Transient Flow Analytical and Numerical Results for Radial Gas Flow with Klinkenberg Effect

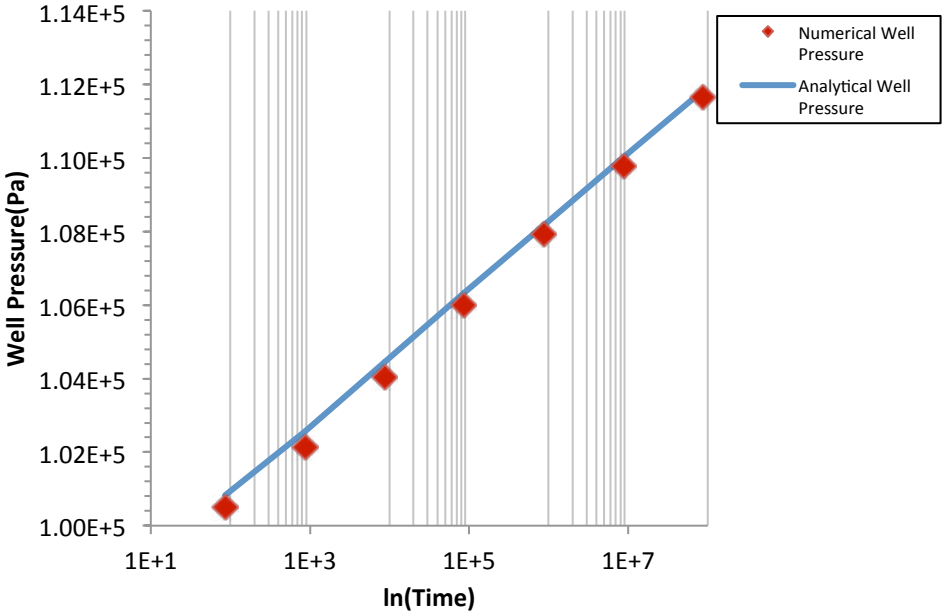

Fig. 6 Transient Flow Analytical and Numerical Results for Radial Gas Flow with Klinkenberg Effect

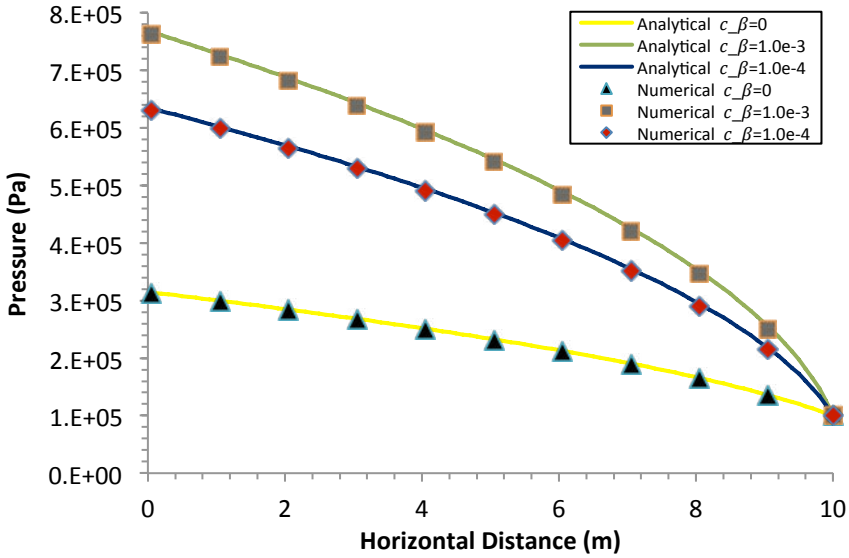

Fig. 7 Steady-State Analytical and Numerical Results for Linear Non-Darcy Gas Flow

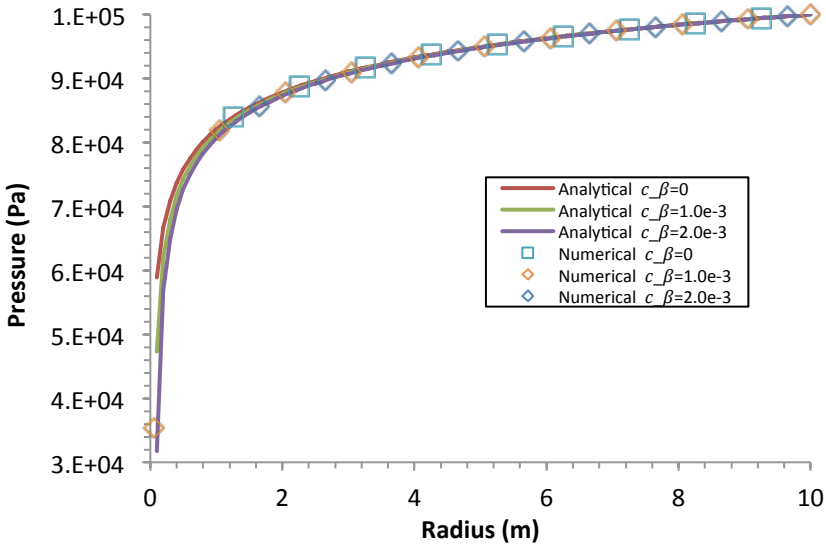

Fig. 8 Steady-State of Analytical and Numerical Results for Radial Non-Darcy Flow

Application

In this section, we demonstrate the use of the proposed mathematical model for modeling gas production from a shale gas reservoir associated with hydraulic fracturing. **Fig. 9** shows the schematic of the level of fracture complexities (Warpinski et al., 2008), which can all be handled by the proposed gas flow model. Here we present the simulation problem of gas flow in a hydraulic fractured well as an example to illustrate the capability of our hybrid fracture modeling approach to capture flow behavior of hydraulic fracture and nature fracture network in these reservoirs.

The system we model includes a single vertical hydraulic fracture in the drainage area of a well in a 3-D setting, and the reservoir is natural fractured. Fluids in the system include gas and water, but water is at residual or immobile, so it is a single gas transient flow problem. To simulate performance of this system using our model, the hydraulic fracture is represented by a discrete fracture with finite conductivity and the naturally-fractured reservoir is described by the double-porosity model. Since the system is symmetric, only a quarter of this hydraulically fractured reservoir system is modeled (**Fig. 10)**. The basic parameter set for the simulation is summarized in **Table 2.**

Table. 2 Parameters for Well Testing Analysis

Parameter	Value	Unit
matrix porosity	$\varphi_m = 0.3$	
natural fracture porosity	$\varphi_{nf} = 0.6$	
hydraulic fracture porosity	$\varphi_{hf} = 0.5$	
matrix permeability	$k_m = 9.87\times10^{-17}$	m^2
natural fracture permeability	$k_{nf} = 1.97\times10^{-12}$	m^2
hydraulic fracture permeability	$k_{hf} = 9.87\times10^{-9}$	m^2
klinkenberg coefficient	$b = 0$	Pa
	$b = 3.4\times10^{6}$	
	$b = 3.4\times10^{7}$	
non-darcy flow constant	$c_\beta = 0$	$m^{1.5}$
	$c_\beta = 6.2\times10^{-6}$	
	$c_\beta = 6.2\times10^{-5}$	
	$\beta = c_\beta/(k^{1.25}\Phi^{0.75})$	
standard gas density	$\rho_{sg} = 0.02$	kg/m^3
gas compressibility factor	$\alpha = 7.08\times10^{-6}$	kg/Pa m^3
gas viscosity	$\mu = 1.64\times10^{-5}$	Pa s
Langmuir volume	$V_L = 0$	m^3
	$V_L = 1.27\times10^{3}$	
	$V_L = 1.27\times10^{4}$	
Langmuir pressure	$P_L = 2.07\times10^{6}$	Pa
formation temperature	$T = 200$	℃
reservoir length	$X = 500$	M
reservoir width	$Y = 500$	M
reservoir thickness	$Z = 5$	m
hydraulic fracture length	$X_{hf} = 40$	m
hydraulic fracture width	$Y_{hf} = 0.02$	m
hydraulic fracture thickness	$Z_{hf} = 5$	m
matrix block thickness	$\Delta L_m = 10$	m
natural fracture volume fraction	$f_{Vnf} = 0.01$	
well radius	$r_w = 0.1$	m
initial reservoir pressure	$P_i = 3.45\times10^{6}$	Pa
initial gas saturation	$S_{gi} = 0.98$	
gas production rate	$Q_g = 2.382\times10^{1}$	m^3/day
	$Q_g = 2.382\times10^{4}$	

Using the simulator, we are able to analyze well testing results of gas wells in unconventional reservoirs with including Klinkenberg effect, non-Darcy flow, and adsorption/desorption terms. Transient flow behavior and type curves simulated are shown in **Fig. 11, Fig. 12**, and **Fig. 13,** in terms of dimensionless pseudo-pressure change and dimensionless time. **Fig. 11** shows pressure transient under Klinkenberg, the large b value, the larger effect on gas permeability, the smaller flow resistance, and the lower pressure drop. Non-Darcy flow behavior is shown in **Fig.12**, indicating that the larger non-Darcy flow coefficient leads to larger flow resistance or large pressure drop at the well.

The effect of adsorption on transient pressure is shown in **Fig. 13**. Adsorption terms tend to slow down the drop of pseudo pressure. This is because with the drop of pressure, more adsorbed gases are released and serve as a source, slowing down the pressure drop, similar to a constatnt pressure boundary condition.

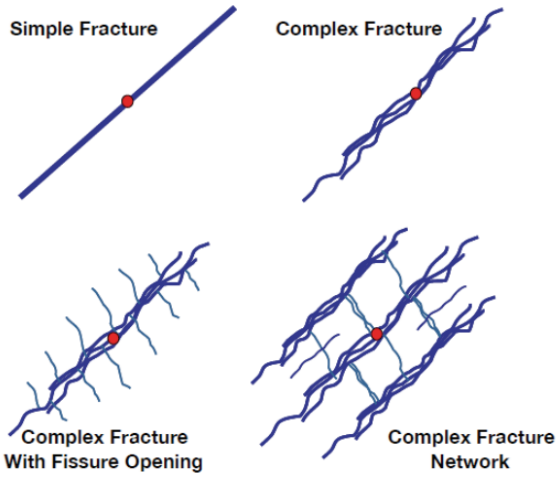

Fig. 9 Schematic of the level of fracture complexities (Warpinski et al., 2008)

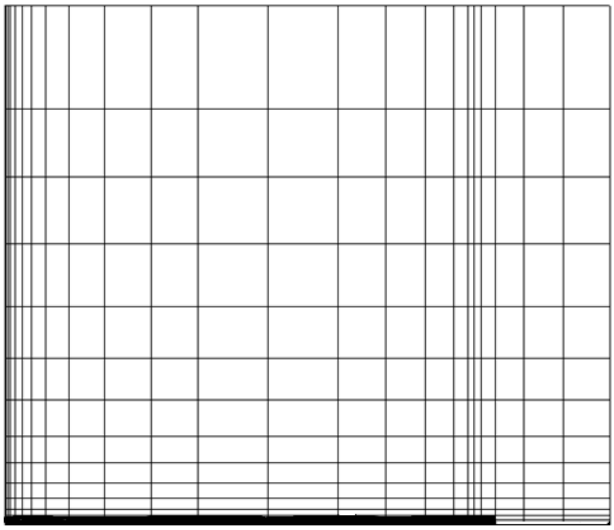

Fig. 10 Configuration of a quarter of the hybrid fracture model of a hydraulically fractured reservoir system

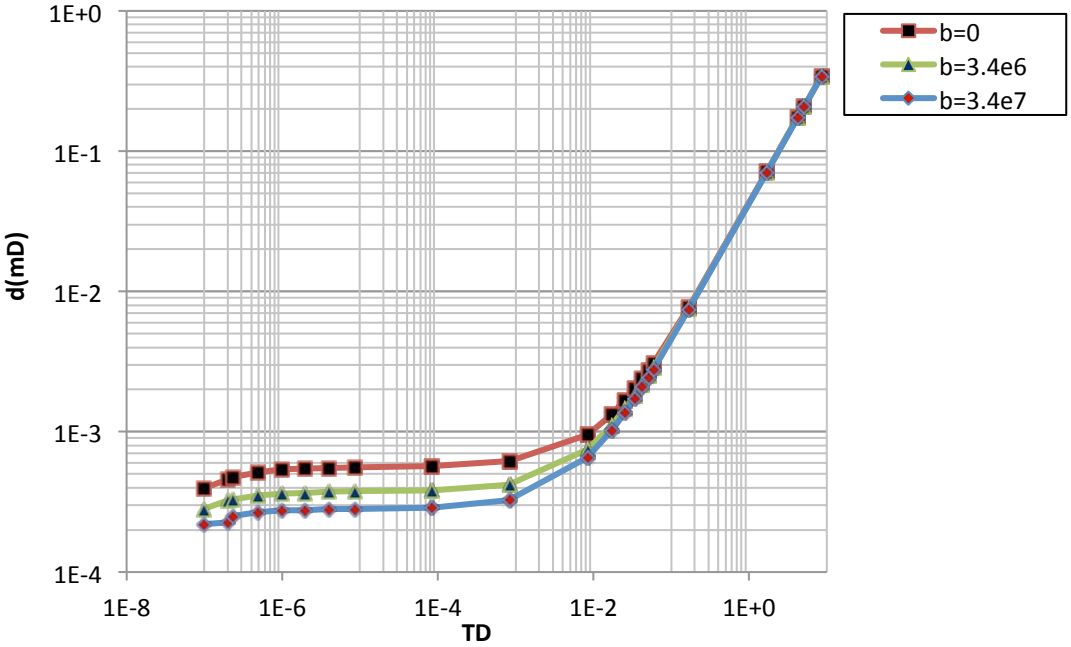

Fig.11 Type curve analysis of Klinkenberg effect (d(mD):Dimentionless Pseudo Pressure Change; TD: Dimentionless Time)

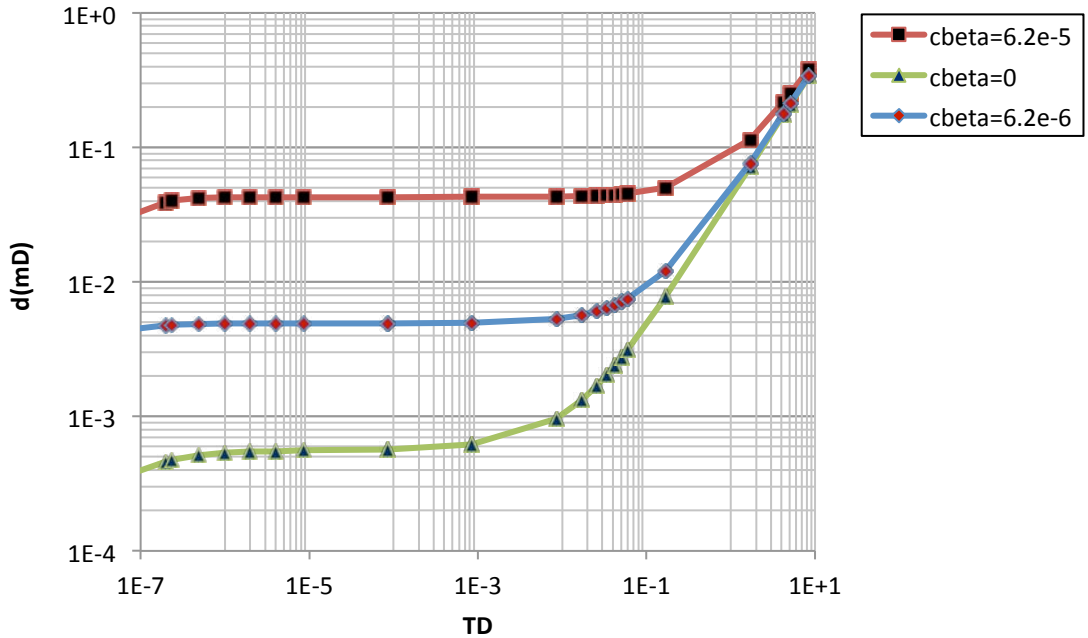

Fig.12 Type curve analysis for non-darcy flow
[d(mD):Dimentionless Pseudo Pressure Change; TD: Dimentionless Time]

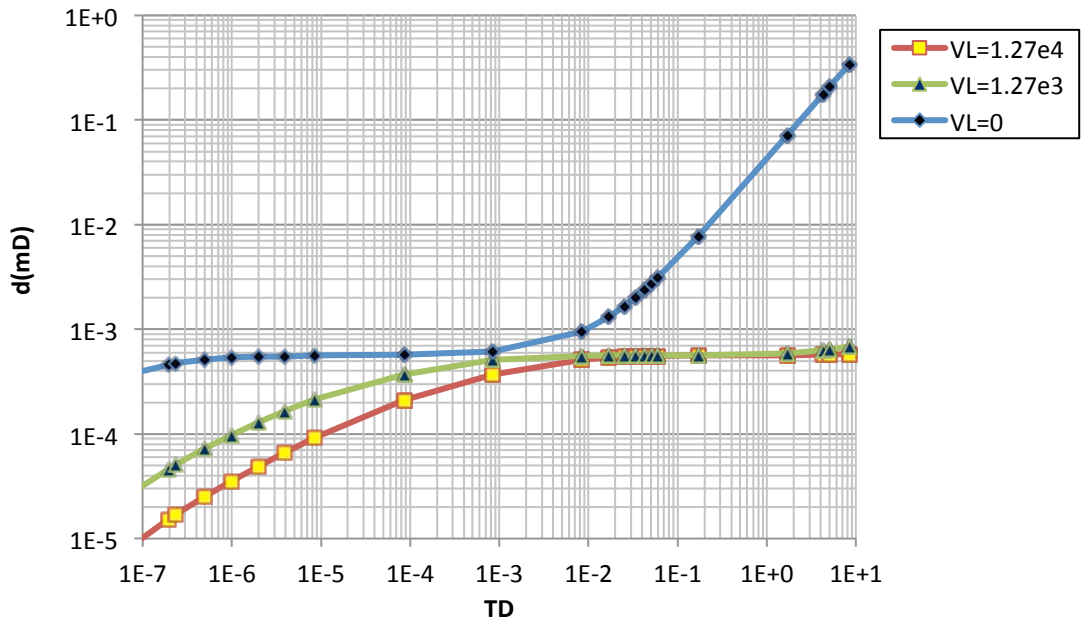

Fig.13 Type curve analysis of adsorption terms
[d(mD):Dimentionless Pseudo] Pressure Change; TD: Dimentionless Time]

Concluding Remarks

In this paper, we present a numerical model for gas and water two-phase flow in unconventional, low-permeability porous or fractured reservoirs of shales or tight formations. The model incorporates several relevant physical processes, such as Klinkenberg effect, non-Darcy flow, and adsorption terms. The proposed mathematical model has been implemented and tested using a multiphase, multidimensional reservoir simulator. In addition, we derive several analytical solutions, which are used to verify the numerical model and its simulation results.

It should be mentioned that the present gas flow model uses on a general multiple-continuum concept, which is able to model various types of reservoir formations and multi-scaled fractures and matrix systems. As application examples, we use the simulator to study and analyze transient pressure responses of gas wells in unconventional reservoirs, realted to Klinkenberg effect, non-Darcy flow, and adsorption/desorption terms.

Appendix A: Derivation of Analytical Solutions for 1-D Steady-State Gas Flow

1. Steady-State Flow with Klinkenberg Effect

Permeability with Klinkenberg effects: $k = k_\infty(1 + \frac{b}{P})$ (1.1)

Mass conservation equation: $\rho v A = Q_m$ (1.2)

Darcy's Law: $v = -\frac{k}{\mu}\nabla P$ (1.3)

Ideal gas equation: $\rho = \alpha P$ (1.4)

1.1 1-D Linear Flow

Under one-dimensional, linear, horizontal, and steady-state flow condition, the boundary conditions are: a constant mass injection rate Q_m is imposed at the inlet (x=0) and the gas pressure is kept constant at the outlet (x=L). Combining equations (1.1) to (1.4), we get:

$$-A\alpha\frac{k_\infty}{\mu}(P + b)\frac{dP}{dx} = Q_m \quad (1.5)$$

Solve this ODE with two boundary conditions and the solution is:

$$P(x) = -b + \sqrt{b^2 + P_L^2 + 2bP_L + \frac{2Q_m\mu(L-x)}{k_\infty A\alpha}} \tag{1.6}$$

1.2 1-D Radial Flow

Under the one-dimensional, radius, horizontal and steady-state flow conditions, the boundary conditions are: a constant mass injection rate Q_m is imposed at the well ($r=r_w$) and the gas pressure is kept at constant, P_e , at the outlet ($r = r_e$). The formation thickness is h. Combining Eqs. (1.1) to (1.4) with in coporation of the well condition, we get:

$$-2\pi rh\alpha\frac{k_\infty}{\mu}(P+b)\frac{dP}{dr} = Q_m \tag{1.7}$$

$$(P+b)\,dP = -\frac{Q_m\mu}{2\pi h\alpha k_\infty}\frac{1}{r}dr \tag{1.8}$$

Solve this ODE of (1.8) with the outer boundary condition:

$$P(r) = -b + \sqrt{b^2 + P_e^2 + 2bP_e + \frac{2Q_m\mu}{2\pi h\alpha k_\infty}\ln\left(\frac{r_e}{r}\right)} \tag{1.9}$$

2 1-D Steady-State Non-Darcy Flow

Mass conservation equation: $\rho vA = Q_m$ (2.1)

Forchheimer flow: $-\nabla P = \frac{\mu}{k}v + \beta\rho v|v|$ (2.2)

Ideal gas equation: $\rho = \alpha P$ (2.3)

2.1 1-D Linear Flow

Under one-dimensional, linear, horizontal and steady-state flow condition, the boundary conditions are: a constant mass injection rate Q_m is imposed at the inlet (x=0), and the gas pressure is kept constant at the outlet (x=L).

From equation (2.2),

$$\beta\rho v^2 + \frac{\mu}{k}v + \frac{\partial P}{\partial x} = 0 \tag{2.4}$$

$$v = \frac{-\frac{\mu}{k} + \sqrt{\left(\frac{\mu}{k}\right)^2 - 4\beta\rho\frac{\partial P}{\partial x}}}{2\beta} \tag{2.5}$$

Substitutibg (2.1) and (2.3) into (2.5), we get:

$$\frac{-\frac{\mu}{k} + \sqrt{\left(\frac{\mu}{k}\right)^2 - 4\beta\rho\frac{\partial P}{\partial x}}}{2\beta} = \frac{Q_m}{A} \tag{2.6}$$

Assume $c_1 = 2\beta\frac{Q_m}{A}$, then we have,

$$c_1 + \frac{\mu}{k} = \sqrt{\left(\frac{\mu}{k}\right)^2 - 4\beta\rho\frac{\partial P}{\partial x}} \tag{2.7}$$

$$\left(c_1^2 + 2c_1\frac{\mu}{k}\right)(L-x) = 2\alpha\beta(P_x^2 - P_L^2) \tag{2.8}$$

The analytical solution is,

$$P_x = \sqrt{\frac{c_1^2 + 2c_1\frac{\mu}{k}}{2\alpha\beta}(L - x) + P_L^2} \tag{2.9}$$

2.2 1-D Radial Flow

Under the one-dimensional, radius, horizontal and steady-state flow conditions, the boundary conditions are: a constant mass production rate Q_m is maintained at the well (r=r_w),, and at the outlet (r=r_e), the gas pressure is kept constant P_e. The reservoir thickness is h.

From equation (2.2), $-\beta\rho v^2 + \frac{\mu}{k}v + \frac{\partial P}{\partial r} = 0$ (2.10)

or,

$$v = \frac{\frac{\mu}{k} - \sqrt{\left(\frac{\mu}{k}\right)^2 + 4\beta\rho\frac{\partial P}{\partial r}}}{2\beta\rho} \tag{2.11}$$

Substituting (2.1) and (2.3) into (2.11), we get:

$$r\frac{\frac{\mu}{k} - \sqrt{\left(\frac{\mu}{k}\right)^2 + 4\beta\rho\frac{\partial P}{\partial r}}}{2\beta} = \frac{Q_m}{2\pi h} \tag{2.12}$$

Assume $c_2 = \frac{\beta Q_m}{\pi h}$,

$$\frac{\mu}{k} - \frac{c_2}{r} = \sqrt{\left(\frac{\mu}{k}\right)^2 + 4\beta\rho\frac{\partial P}{\partial r}} \tag{2.13}$$

$$\left(\frac{\mu}{k}\right)^2 + \left(\frac{c_2}{r}\right)^2 - 2\frac{\mu}{k}\frac{c_2}{r} = \left(\frac{\mu}{k}\right)^2 + 4\beta\rho\frac{\partial P}{\partial r} \tag{2.14}$$

$$\left(\frac{c_2^2}{r^2} - \frac{2c_2\mu}{kr}\right)dr = 4\alpha\beta P\, dP \tag{2.15}$$

Solving the ODE above, we get:

$$-c_2^2\left(\frac{1}{r_e} - \frac{1}{r}\right) - \frac{2c_2\mu}{k}\ln\left(\frac{r_e}{r}\right) = 2\alpha\beta(P_L^2 - P^2) \tag{2.16}$$

Or the final solution,

$$P = \sqrt{P_L^2 - \frac{c_2^2}{2\alpha\beta}\left(\frac{1}{r} - \frac{1}{r_e}\right) + \frac{c_2\mu}{k\alpha\beta}\ln\left(\frac{r_e}{r}\right)} \tag{2.17}$$

Acknowledgments

This work was supported in part by Colorado School of Mines and in part RIPED by PetroChina Inc. of China.

Nomenclature

A_{ij}	interface areas between two gridblock i and j (m^2)
b	Klinkenberg factor (Pa)
D	depth from a datum, m
$\mathrm{flow}_{\beta,ij}$	mass flow of fluid β (kg/s/m^2) along connection ij of time level n+1
$\mathrm{flow}^{k}_{\beta,ij}$	mass flow of component k in fluid β (kg/s/m^2) along connection ij of time level n+1
g	gravitation constant (m/s^2)
G	threshold pressure or potential gradient (Pa/m)
k	absolute permeability of porous media (m^2)
$k_{r\beta}$	relative permeability to phase β
k_∞	absolute permeability at large gas pressure
P	Pressure (Pa)
P_β	pressure of phase β (Pa)
q_β	source/sink - or fracture matrix interaction of mass for phase β (kg/s m^3)
Q^{n+1}_β	source/sink or fracture-matrix exchange terms for phase β (kg/s) of time level n+1
R^{k}_β	residual term of mass balance of phase β (kg/m^3) of time level n+1
S_β	fluid saturation of phase β
t	time (s)
Δt	time step (s)
V_i	volume of gridblock i (m^3)
$\mathbf{v}_\beta$	Darcy's or volumetric velocity of phase β (m/s)
Z_i	depth of the center of block i from a datum, m

Greek Symbols

β_β	effective non-Darcy flow coefficient for phase β (m^{-1}) of
ϕ	effective porosity of formation
Φ_β	flow potential (Pa)
γ_{ij}	transmissivity (m^3)
$\bar{\gamma}_{ij}$	transmissivity for non-Darcy flow (m^{-1})
$\lambda_{\beta,ij+1/2}$	mobility of phase β between gridblcoks i and j
μ_β	viscosity of phase β (Pa•s)
ρ_β	density of phase β at *in situ* conditions (kg/m^3)

Subscripts

g	gas
i	gridblock i
j	gridblock j
β	index of fluid phase

Superscripts

k	index for mass components.
n	previous time level n
n+1	current time level n+1
p	iteration level

References

Alana Leahy-Dios, Mlta Das, Anshul Agarwal, Robert D. Kaminsky, SPE 147352, presented at the SPE Annual Technical Conference, Denver, Colorado, 30 Octomber-2 November 2011

Bybee, K., Horizontal wells in tight gas sands: risk management to maximize success, *JPT*, 61-63, October, 2008.

Cippolla, C. L., E. P. Lolon, J. C. Erdle, and V. Tathed, Modeling Well Performance in Shale-Gas Reservoirs, SPE 125532, presented at the 2009 SPE/EAGE Reservoir Characterization and Simulation Conference, Abu Dhabi, UAE, 19-21 October, 2009.

Denney, D., Rock type-understanding productivity in tight gas sands, *JPT,* 53-56, October, 2008.

Gong, Bin, Guan Qin, Brian F. Towler, and Hongyan Wang, Discrete Modeling of Natural and Hydraulic Fractures in Shale-Gas Reservoirs, SPE Annual Technical Conference and Exhibition, Denver, Colorado, USA, 30 October-2 November 2011

Forsyth, P. A., Y. S. Wu and K. Pruess, Robust Numerical Methods for Saturated-unsaturated Flow with Dry Initial Conditions in Heterogeneous Media. Advance in Water Resources 18, p. 25-38, 1995.

Kelkar M. and M. Atiq, Upgrading Method for Tight Gas Reservoirs, SPE 133301, presented at the SPE Annual Technical Conference and Exhibition, Florence, Italy, 19-22 September, 2010.

King, E. G., Thirty Years of Gas Shale Fracturing: What Have We learned?, SPE 133456, presented at the SPE Annual Technical Conference and Exhibition, Florence, Italy, 19-22 September, 2010.

Klinkenberg, L.J., The Permeability of Porous Media to Liquids and Gases, in API Drilling and Production Practice, 200–213, 1941.

Langmuir Irving, The constitution and fundamental properties of solids and liquids. Journal of the American Chemical Society 38 (11): 2221–2295,1916

Lei, Qin, Wei Xiong, Jiangru Yuan, Yuquan Cui, and Yu-Shu Wu, Analysis of Stress Sensitivity and Its Influence on Oil Production from Tight Reservoirs, SPE-111148, presented at the 2007 SPE Eastern Regional Meeting held in Lexington, Kentucky, U.S.A., 17–19 October 2007.

Mirzaei, M. and C.L. Cipolla, Schlumberger, A Workflow for Modeling and Simulation of Hydraulic Fractures in Unconventional Gas Reservoirs, SPE Middle East Unconventional Gas Conference and Exhibition, Abu Dhabi, UAE, 23-25 January 2012

MIT, The future of natural gas – an interdisciplinary MIT study, 2010.

Pruess, K., C. Oldenburg and G. Moridis, *TOUGH2 User's Guide, Version 2.0,* Report LBNL-43134, Berkeley, California: Lawrence Berkeley National Laboratory, 1999.

Shabro,V. C. Torres-Verdín, and F. Javadpour," Numerical Simulation of Shale-Gas Production: From Pore-Scale Modeling of Slip-Flow, Knudsen Diffusion, and Langmuir Desorption to Reservoir Modeling of Compressible Fluid", SPE 144355. North American Unconventional Gas Conference and Exhibition, The Woodlands, Texas, USA, 14-16 June 2011

Severino Jose G., SPE, Cimarex Energy; Luis E. Gomez, Shoubo Wang, Ram S. Mohan, and Ovadia Shoham, Mechanistic "Modeling of Solids Separation in Solid/Liquid Hydrocyclones," in SPE Projects, Facilities & Construction, Vol. 5, No. 3, September 2010

Silin, Dmitriy and Tim Kneafsey, Gas Shale: From Nanometer-scale Observations tp Well Modeling, CSUG/SPE 149489, presented at the Canadian UnconventionalResourcesConference, Calgary, Alberta, Canada, 15-17 November, 2011.

Warpinski, N. R., M. J. Mayerhofer, M. C. Vincent, C. L. Cipolla, and E. P. Lolon, Stimulating Unconventional Reservoirs: Maximizing Network Growth While Optimizing Fracture Conductivity, presented at the 2008 SPE Shale Gas Production Conference, Fort Worth, Texas, 16-18 November, 2008.

Wu, Y.S. and P. Fackahroenphol, "A Unified Mathematical Model for Unconventional Reservoir Simulation," SPE-142884, presented at the SPE EUROPEC Conference, to be held from 23-26 May 2011 in Vienna, Austria, 2011

Wu, Y.S. G. Moridis, B. Bai, and K. Zhang, A Multi-Continuum Model for Gas Production in Tight Fractured Reservoirs, SPE 118944, Prepared for presentation at the 2009 SPE Hydraulic Fracturing Technology Conference held in The Woodlands, Texas, USA, 19–21 January 2009.

Wu, Y.S., Numerical simulation of single-phase and multiphase non-Darcy flow in porous and fractured reservoirs, Transport in Porous Media, Vol. 49, No. 2, 209-240, 2002

Wu, Y.S. A virtual node method for handling wellbore boundary conditions in modeling multiphase flow in porous and fractured media, Water Resources Research, 36 (3), 807-814, 2000.

Wu, Y.S. and K. Pruess "A numerical method for simulating non-Newtonian fluid flow and displacement in porous media", Vol. 21, Advances in Water Resources, 351-362, 1998.

Wu, Y.S., K. Pruess, and P. Persoff, "Gas Flow in Porous Media with Klinkenberg Effects," Transport in Porous Media, Vol.32, 117-137, 1998.

Wu, Y. S., K. Pruess, and P.A. Witherspoon, "Flow and Displacement of Bingham Non-Newtonian Fluids in Porous Media," SPE Reservoir Engineering, pp.369-376, 1992

Wu, Y. S., and K. Pruess, A multiple-porosity method for simulation of naturally fractured petroleum reservoirs, SPE Reservoir Engineering, 3, 327-336, 1988.

Xiong, Wei, Qun Lei, Jiangru Yuan, Shusheng Gao, and Yu-Shu Wu, "Behavior of Flow through Low-Permeability Reservoirs," SPE-113144, prepared for presentation at the 2008 SPE EUROPEC Conference to be held in Rome, Italy, 9-12 June 2008